Sustainable Food Technology

ROYAL SOCIETY OF CHEMISTRY

PAPER

View Article Online
View Journal | View Issue

Cite this: *Sustainable Food Technol.*, 2025, **3**, 1053

Sustainable liposomal delivery of *Centella asiatica* polyphenols: β-sitosterol stabilization, LC-MS/MS profiling, and simulated release study

Soubhagya Tripathy * and Prem Prakash Srivastav

This study investigates the influence of β-sitosterol (βS) on the structural characteristics, physicochemical stability, and *in vitro* release behavior of liposomes encapsulating *Centella asiatica* leaf extract (CALE). Additionally, the retention kinetics of bioactive compounds were analyzed using a first-order equation alongside assessments of thermal stability and lipid oxidation. The polyphenolic composition of CALE was characterized through LC-MS/MS in both positive and negative ionization modes, revealing the presence of several key compounds with distinct retention times. Findings indicated that the highest encapsulation efficiency (74.789 ± 0.811%) was achieved when the soy lecithin (SL) to β-sitosterol (βS) ratio was 7 : 3 (LP-βS (C3)). The particle size of all formulations remained under 700 nm, with a retention rate exceeding 50% after 28 days of storage. FTIR analysis confirmed the absence of interactions between polyphenols and the encapsulating material, validating the successful encapsulation of bioactive compounds. Furthermore, simulated release studies demonstrated that encapsulation enhanced the bioavailability of CALE bioactive compounds in liposomes. These findings suggest that βS is a viable and promising approach for developing cholesterol-free, bioactive-enriched liposomal formulations suitable for functional food applications.

Received 31st March 2025
Accepted 14th May 2025

DOI: 10.1039/d5fb00127g

rsc.li/susfoodtech

Sustainability spotlight

This study highlights a sustainable approach to enhancing the bioavailability and stability of *Centella asiatica* bioactive compounds (BACs) using ultrasound-assisted extraction and liposomal encapsulation. This research aligns with the United Nations Sustainable Development Goals (SDGs) by promoting sustainable food innovation (SDG 9: Industry, Innovation, and Infrastructure) and good health and well-being (SDG 3) through the development of bioactive-enriched liposomal formulations. By utilizing β-sitosterol as a plant-based stabilizer, the study supports sustainable production practices (SDG 12: Responsible Consumption and Production) and reduces dependence on cholesterol-based liposomes. Additionally, this work fosters green chemistry principles by integrating natural bioactive compounds and lipid-based delivery systems, advancing eco-friendly and health-conscious food processing solutions for a sustainable future.

1 Introduction

Bioactive compounds are functional molecules with significant therapeutic potential, contributing beyond essential nutrition.[1,2] These compounds are naturally found in various food sources, including fruits, vegetables, whole grains, and medicinal plants.[3] For example, *Centella asiatica* (CA) is abundant in bioactive constituents such as phenolic compounds, triterpenoids, volatile oils, vitamins, and minerals.[4–6] Consuming CA bioactive compounds has been linked to numerous health benefits, including reduced cancer risks, diabetes, cardiovascular diseases, stroke, and age-related degeneration.[7] However, challenges such as poor aqueous solubility, instability during processing, and low bioavailability hinder their practical applications. Therefore, developing effective preservation strategies for bioactive compounds (BACs) is essential.

Encapsulation is a well-established approach for incorporating bioactive compounds into a protective matrix, regardless of their physical state. Nanotechnology represents a cutting-edge and rapidly evolving field that plays a crucial role in minimizing particle size, enhancing sensory attributes, and extending the shelf life of food products.[8,9] The growing consumer preference for healthier and naturally derived food products has sparked significant interest in substituting synthetic additives with bioactive compounds of natural origin. Nanoencapsulation serves as a practical approach to incorporating biologically active molecules, particularly those that are lipophilic or poorly soluble in water, into functional food systems.[10,11] Among various encapsulation techniques, liposome-based delivery systems have gained prominence in

Department of Agricultural and Food Engineering, Indian Institute of Technology Kharagpur, Kharagpur, West Bengal 721302, India. E-mail: mr.soubhagyatripathy@gmail.com; Tel: +91-8457829200

the fields of pharmaceuticals, cosmetics, and food due to their advantageous characteristics, including "biocompatibility, biodegradability, non-toxicity, and non-immunogenicity".[12] Liposomes (LPs) are lamellar vesicles with an internal aqueous core surrounded by one or more concentric phospholipid bilayers. This unique structure allows them to encapsulate bioactive compounds of varying solubilities, including hydrophilic, hydrophobic, and amphiphilic molecules. In addition to improving delivery efficiency, the interaction between encapsulated bioactive compounds and liposomal structures may enhance their functionality upon ingestion.[13]

Lecithin, a natural compound extracted and purified primarily from egg yolk and soybeans, has gained attention for its pharmacological properties. Rich in phospholipids, it presents a more economical and readily available alternative to synthetic counterparts.[14] Studies have highlighted its synergistic effects when combined with phenolic compounds and sterols. Due to its water-insoluble nature, lecithin is particularly well-suited for formulations requiring extended stability.[15] Cholesterol plays a crucial role in regulating the properties of bio-membranes. In order to circulate within the plasma, cholesterol must associate with carrier molecules such as lipoproteins or albumin. Based on their density, size, and the composition of structural and associated proteins, lipoproteins are mainly classified into low-density lipoproteins (LDL) and high-density lipoproteins (HDL).[16] Drawing inspiration from this natural function, cholesterol is commonly incorporated into liposomal formulations to enhance membrane stability, functioning similarly to "rebars" in construction.[17] However, excessive dietary cholesterol intake has been associated with elevated low-density lipoprotein (LDL) cholesterol levels, commonly known as 'bad' cholesterol.[18] Increased LDL cholesterol contributes to the buildup of plaque in arterial walls, a condition known as atherosclerosis, which significantly raises the risk of cardiovascular diseases.[19] Therefore, the long-term consumption of cholesterol-rich liposomes in dietary applications may pose health concerns by potentially elevating LDL cholesterol levels. In contrast, β-sitosterol (βS), a plant-derived sterol or phytosterol, is widely recognized for its LDL cholesterol-lowering effects and is a natural "antioxidant" in food.[20,21] Beyond its ability to reduce cholesterol levels, β-sitosterol exhibits various biological activities, including antitumor, antioxidant, antidiabetic, anti-inflammatory, and gallstone-preventing effects, and may also alleviate prostatitis symptoms.[22] Notably, β-sitosterol shares a similar structural framework with cholesterol, essential for modulating membrane properties.[23]

This study aims to extract, characterize, and encapsulate bioactive compounds from *Centella asiatica* using soy lecithin (SL) and β-sitosterol (βS) liposomes to improve their stability and regulate their release. The research emphasizes the characterization of encapsulated particles, assessing their retention and stability under various storage conditions, and examining their behaviour during *in vitro* digestion. The findings will support the development of an efficient liposomal delivery system to enhance the bioavailability and functionality of *Centella asiatica* bioactive compounds for potential applications in the food, pharmaceutical, and nutraceutical industries.

2 Materials and methods

2.1. Reagents used

L-α-Phosphatidylcholine (PC, derived from soybean, purity >30%) was obtained from HiMedia Laboratories. Chemicals such as sodium phosphate monobasic anhydrous (99%), sodium phosphate dibasic dodecahydrate (98.5%), Folin–Ciocalteu reagent (FCR), and β-sitosterol (soybean-derived) were sourced from Sisco Research Laboratories Pvt. Ltd (SRL). Analytical-grade solvents and reagents, including ethanol, methanol, thiobarbituric acid (TBA), trichloroacetic acid, acetonitrile, formic acid, chloroform, and hydrochloric acid (HCl), were used in the study. All solutions were prepared using distilled water (DW).

2.2. Sample preparation

Centella asiatica leaves were freshly obtained from the Technology Market at IIT Kharagpur, India, in the morning during the rainy season of August. The leaves were carefully detached from the stems and thoroughly rinsed with tap water to remove any external contaminants. Prior to further processing, they were uniformly spread on a plate and left at room temperature for 30 min to facilitate the evaporation of surface moisture.

2.3. Extraction of CALE BACs using ultrasound

The leaves were dried in a recirculatory hot air dryer at 40 °C for 4 h until a constant weight was achieved (9.241 ± 1.014% db). Using a mechanical grinder, the dried leaves were ground into a fine powder (80 mesh size). The powdered material was extracted using a "Hielscher ultrasonic processor (UP50H)" with "62% ethanol at room temperature", maintaining a "solid-to-solvent ratio of 1 : 23 (w/v)". The transducer functioned at a power of 50 W and a frequency of 30 kHz.[24,25] The obtained extract was centrifuged at 4 °C for 10 minutes at 9000 rpm. The supernatant was then filtered using Whatman No. 1 filter paper, and the solvent was removed through rotary evaporation under vacuum at 45 °C. Finally, stored at −20 °C after freeze–drying (FD-CALE) at −40 ± 2 °C and pressure of 150 mbar for future use.

2.4. Identification of CALE BACs using LC-MS/MS

The LC-MS/MS analysis of CALE was performed using a Waters2695 liquid chromatograph in conjunction with an Agilent G1946D quadrupole mass spectrometer (Agilent Technologies, Waldrom, Germany). Data collection and processing were carried out using "MassLynx 4.1 software". Compound separation was achieved using a "reversed-phase XTerra MS C18 column" ("2.1 × 100 mm, 2.5 μm particle size"). The analytical approach was modified by Singh *et al.*[26] The "mobile phase" was composed of solvent A (0.1% formic acid in water) and solvent B (acetonitrile), and gradient elution was applied as follows: 0–6 min (0–2% B), 6–14 min (2–5% B), 14–20 min (5–10% B), and 20–30 min (25–30% B). The system operated at a "constant flow rate of 0.4 mL min^{-1}", with a maintained "temperature of 25 °C".

2.5. Encapsulation of CALE BACs in liposome

Vesicles were prepared using the TFH method, as outlined by Prevete *et al.*[27] Initially, SL and βS were precisely dissolved in EtOH at different ratios. The organic phase was then subjected to rotary evaporation at 45 °C, forming a thin lipid film. This dried lipid layer was subsequently hydrated using a phosphate-buffered saline (PBS) solution (pH 7.4, 0.01 M) containing FD-CALE (1 mg mL^{-1}) while maintaining continuous orbital agitation, promoting liposome formation. The suspension was further processed using a homogenizer to achieve a uniform dispersion. For comparison, LPs were also synthesized without incorporating βS.

2.6. Characterization of liposomes

2.6.1. Particle size, PDI and zeta potential analysis. The "vesicle size", "polydispersity index (PDI)", and "zeta potential (ζ)" were determined using "dynamic light scattering (DLS)" with a Malvern Zetasizer ZS90 (Malvern Instruments, Worcestershire, UK). To minimize the impact of multiple scattering, the liposomal dispersions were diluted with distilled water at a 1 : 100 ratio. All analyses were performed in triplicate at 25 °C at the scattering angle of 90 °C.[28]

2.6.2. Encapsulation efficiency (EE). The LPs were isolated through centrifugation at 12 000×*g* for 180 minutes at 20 °C, following the method described by Hashim *et al.*[29] The resulting supernatant, which contained non-encapsulated phenolic compounds, was collected for analysis. To quantify the encapsulated phenolic compounds, the resuspended liposomes were treated with a 1 : 1 (v/v) mixture of methanol and chloroform. The mixture was vigorously vortexed to promote phase separation. The phenolic content in both the upper water–methanol phase and the supernatant was quantified following the method described by Tripathy and Srivastav.[30] These values were then utilized to calculate the encapsulated and non-encapsulated fractions, and the EE was measured using eqn (1).

$$\mathrm{EE}(\%) = \frac{A_2 - A_1}{A_2} \times 100 \quad (1)$$

where, A_1 = non-encapsulated phenolic compounds A_2 = encapsulated + non-encapsulated phenolic compounds.

2.6.3. FTIR analysis. Each sample, including soy lecithin, β-sitosterol, empty liposomes (LP), and LP-βS (C3), was mixed with potassium bromide (KBr). The pellets formed were analyzed using a "FTIR spectrometer (NICOLET 6700, Thermo Fisher Scientific, USA)". The "FTIR spectra" were recorded within the 4000–400 cm^{-1} wavelength range.

2.6.4. SEM analysis. The morphology and surface characteristics of the encapsulated particles were analyzed using a "scanning electron microscope (ZEISS EVO 60)" integrated with an "Oxford EDS detector (Carl ZEISS SMT, Germany)". The samples were mounted onto cylindrical holders and placed on aluminum stubs, then coated with a thin gold layer (approximately 25 nm) using a sputter coater (Quorum Q150R ES, USA) prior to scanning *via* scanning electron microscopy (SEM).

2.7. Retention of bioactive compounds

The "total phenolic content (TPC)" of FD-CALE and LP-βS (C3) was determined using a spectrophotometric approach with the Folin–Ciocalteu reagent (FCR), as described by Tripathy and Srivastav.[30] The samples were kept at 4 °C and 27 °C for 28 days and analyzed every seven days in triplicate. The "retention rate (%)" was calculated using the following eqn (1):

$$\text{Retantion rate } (\%) = \frac{\text{total TPC in LP\_βS (C3)}}{\text{total TPC in leafextract}} \quad (2)$$

2.7.1. Kinetics of bioactive retention rate. The degradation of total phenolic content (TPC) adhered to first-order kinetics. Consequently, a "first-order kinetic model" fitted the phenolic degradation during storage. This model can be mathematically represented as follows:[31,32]

$$\ln Q = \ln Q_0 - k_t \quad (3)$$

$$t_{1/2} = \frac{\ln 2}{k} \quad (4)$$

$$D = \frac{1}{k} \quad (5)$$

where, "Q represents the phenolic compound at a given time (t), while Q_0 denotes their initial concentration. The parameter k corresponds to the rate constant, and $t_{1/2}$ signifies the half-life of the phenolic compound and antioxidant activity. Additionally, the D value indicates the duration required for a 90% reduction in the bioactive compound concentration".

2.8. Stability study

2.8.1. Thermal stability. The thermal stability of LP-βS (C3) was evaluated using a modified version of the method outlined by Tai *et al.*[22] LPs were transferred into test tubes and subjected to heat treatment in a water bath under three specific temperature–time conditions: 35 °C for 6 hours, 65 °C for 25 minutes, and 90 °C for 30 seconds. The retention rate was calculated using the following formula:

$$\text{Rentation rate } (\%) = \frac{C_t}{C_0} \times 100 \quad (6)$$

where C_0 and C_t represent concentrations of phenolics in the initial and at different time temperature combination (LP-βS (C3)), respectively.

2.8.2. Lipid oxidation. The level of malondialdehyde (MDA), a secondary product of lipid peroxidation, was quantified following the thiobarbituric acid (TBA) method outlined by Fan *et al.*[33] Under acidic conditions and elevated temperatures, MDA reacts with TBA, producing a red-brown chromogenic complex that exhibits maximum absorbance at 532 nm. Absorbance readings were taken at 532 nm to measure the MDA concentration in liposomes, with blank liposomes serving as the reference. The MDA content was then calculated using the following formula:

$$\text{TBARS (μg MDA eq. per mg of sample)} = \frac{A_c \times V}{W} \quad (7)$$

where, "A_c = amount of 1,1,3,3-tetraethoxypropane (μg mL^{-1}), V = total volume (mL), and W = sample weight taken (mg)".

2.9 *In vitro* release behavior of encapsulated particle

Lyophilized PSPE, encapsulated and non-encapsulated, with and without a chitosan coating, underwent an *in vitro* digestion process that mimicked oral, gastric, and intestinal phases, following the method described by Hashim *et al.*[29] The digestion was carried out at 37 °C with continuous shaking at 50 rpm, sequentially using simulated salivary fluid (SSF), simulated gastric fluid (SGF), and simulated intestinal fluid (SIF).

2.10. Statistical analysis

The standard deviation was determined based on data obtained from three separate experiments. To compare the means with a 95% confidence interval, the Tukey test was performed using IBM SPSS Statistics version 22. The model's goodness of fit was assessed through R^2, adjusted R^2, and AIC values. Graphical representations were created using Origin 2023b.

3 Results and discussion

3.1 Identification of bioactive compounds using LC-MS/MS

The LC-MS/MS full "scan and total ion chromatograms" recorded in both "positive and negative" ionization modes. A thorough examination of the base peak and MS/MS fragment patterns obtained from the "LC-MS/MS" analysis enabled the identification of various chemical constituents, including triterpenoids from *Centella asiatica* and several phenolic acids and flavonoids. The principal components detected in the ethanolic extract of *Centella asiatica* are summarized in Tables 1 and 2. In the "LC chromatogram", a peak with a "retention time (R_T)" of 8.45 minutes was attributed to the presence of three isomeric compounds—"chlorogenic acid, crypto-chlorogenic acid, or neo-chlorogenic acid"—based on the observed $[M - H]^-$ ion at m/z 352.82 and a "fragment ion" at m/z 191.06, indicating the "loss of the caffeoyl moiety ($[M–C_9H_7O_3]$)" in its "MS/MS spectrum". These "isomeric phenolic acids", collectively referred to as "caffeoylquinic acids (CQAs)", have been previously identified as key bioactive compounds in *Centella asiatica*, as reported by Long *et al.*, Alqahtani *et al.*, and Abas *et al.*[34–36] Additionally, "dicaffeoylquinic acid (DCQA)" was detected at R_T 22.48 minutes, based on its "$[M - H]^-$ ion" at m/z 514.81 and a "fragment ion" at m/z 191.06, consistent with findings reported by Oszmiański *et al.*[37] Peaks corresponding to possible derivatives of "DCQAs" have also been previously documented as active constituents of *Centella asiatica*.[38] Both positive and negative ionization modes were utilized to analyze "flavonoid glycosides" and their corresponding "aglycones", though the "negative mode" demonstrated greater efficiency in detecting flavonoids within the extract.

Kaempferol and Quercetin were the predominant "flavonoids" identified in the extract. The peak observed at R_T 19.95 min displayed an $[M - H]^-$ ion at m/z 300.81, indicating the presence of Quercetin, which was further confirmed by the loss of a $C_8H_6O_2$ (ring B) fragment. Likewise, the peak at R_T 30.74 min, exhibiting an $[M - H]^-$ ion at m/z 284.87, was

Table 1 Identification of bioactive compounds present in *Centella asiatica* leaves by LC-MS/MS $[M - H]^-$ fraction

Retention time (R_T)	$[M - H]^-$	MS	Compound identified
1.331	190.91	160.84, 119.80	Bornyl acetate
8.499	352.82	191.06	CQA isomer
17	269.06	—	Coutaric acid
17.97	426.99	—	Kaempferol-3-rhamnoside
19.95	476.85	301	Quercetin-3-*O*-glucuronide
19.95	300.81	—	Quercetin
21.26	352.84	191.06	CQA isomer
21.48	460.79	285	Kaempferol-3-*O*-glucuronide
22.48	514.81	353	Di-*O*-caffeoylquinic acid derivatives
23.02	394.94	229.28, 183.04, 159.04	Campesterol
23.49	600.84	301.06	Rutin
24.101	600.84	301.06	Rutin
24.708	975.59	191.06	Madecassoside
25.636	959.52	577.14, 361.19	Asiaticoside
27.17	959.52	577.14, 361.19	Asiaticoside
30.74	284.87	229.28, 150.04, 143.03	Kaempferol
36.63	503.049	503.34	Madecassic acid
39.19	487.107	487.34	Asiatic acid
40.84	248.92	—	Difucol
45.65	276.99	—	Cyanidin
49.08	253.04	—	Chrysin
50.14	277.03	—	Cyanidin
52.52	255.077	—	Apigeninidin
53.06	281.104	—	Damnacanthal
56.36	283.08	133.01	Catechin
57.85	316.79	179	Cafeogltartaric

Table 2 Identification of bioactive compounds present in *Centella asiatica* leaves by LC-MS/MS $[M - H]^+$ fraction

Time	$[M - H]^+$	MS	Compound identified
0.15	195.81	—	Ferulic acid
1.27	542.67	—	Oleuropein
8.82	162.65	—	P-coumaric acid
12.11	392.86	—	Piceid
18.96	468.89	—	Flavone glycoside
19.94	302.66	—	Flavanol
21.54	286.68	229.28, 150.04, 143.03	Kaempferol
22.102	250.66	—	Difucol
25.47	452.85	—	Kaempferol-3-glycoside
26.50	490.88	487.34	Asiatic acid
27.12	200.07	—	Xantoxylin
30.46	531.08	—	Demethyloleuropein
36.69	450.88	—	Luteolin-7-glucosidee
38.07	270.03	144	Flavanone
38.733	269.91	144	Flavanone
40.80	698.89	623, 241, 625	Cyanidin-3-rutinoside
41.61	336.55	163, 181	Hydrocaffeic acid
43.21	519.95	163, 347, 355, 377, 539	Caffeoylquinic acid
45.22	297.806	171, 153	Easters of gallic acid
46.55	341.82	136	Coumaroylquinic acid
52.61	404.83	—	Mallotophenone
53.204	592.88	303, 595, 617	Quercetin-3-*O*-birhamnoside
54.604	453.95	289, 139	Gallocatechin-3-gallate
56.39	453.95	289, 139	Gallocatechin-3-gallate

attributed to Kaempferol, as evidenced by the "loss of $C_8H_6O_2$ (ring B) and $C_4H_4O_2$ (ring A) radicals". Additionally, the flavonoid glycoside rutin was identified at R_T 23.49 and 24.1 min with an $[M - H]^-$ ion at m/z 600.84 and "fragment ions" at m/z 301.06. Other flavonoids detected included kaempferol-3-rhamnoside (R_T 17.97 min), quercetin-3-*O*-glucuronide (R_T 19.95 min), and kaempferol-3-*O*-glucuronide (R_T 21.48 min). These findings align with those reported by Zakaria *et al.*[39]

Numerous studies have indicated that *Centella asiatica* is rich in phytochemicals, particularly triterpenoid saponins such as "asiaticoside and madecassoside", along with their corresponding "aglycones, asiatic acid, and madecassic acid".[38] Asiatic acid and madecassic acid corresponded to peaks at retention times (R_T) of 39.19 min and 36.63 min, exhibiting $[M - H]^-$ ions at m/z 487.107 and 503.049, respectively. "Asiaticoside and madecassoside" were detected at R_T 25.636 min (m/z 959.52) and 24.708 min (m/z 975.59). Another triterpenoid saponin, brahminoside, was identified at R_T 53.204 min with an $[M - H]^+$ ion at m/z 592.88. These findings confirm that *Centella asiatica* is a valuable source of diverse bioactive compounds with significant medicinal potential.

3.2. Characterization of encapsulated particles

The size of particles significantly influences the "stability, encapsulation efficiency, and release properties of bioactive compounds". Generally, smaller particles with a "lower dispersion index" suggest that encapsulated LPs possess enhanced stability and uniformity.[40] Table 3 presents the properties of liposomes (LPs) containing varying amounts of β-sitosterol (βS), with the average particle diameter ranging from 443.738 to 692.695 nm. An increase in βS concentration led to a rise in particle size, primarily due to the spatial occupation within the membrane and the enhancement of lipid bilayer rigidity. This effect occurs as the shorter hydrocarbon chains of βS interact with the hydrocarbon regions near the phospholipid head groups, influencing the membrane structure.[17]

The PDI is another critical parameter that indicates liposomal dispersions' size distribution and stability. A PDI value below 0.3 suggests a "narrow size distribution, high stability, and homogeneity", making the formulation suitable as a carrier for bioactive molecules.[41] The study observed a direct correlation between PDI and βS content, where an equal ratio of soy lecithin (SL) to βS resulted in a PDI of 0.267 ± 0.003, suggesting incomplete homogeneity in dispersion. Additionally, increasing βS content contributed to higher turbidity in LPs, likely due to enhanced light scattering from larger particles. These findings align with previous research.[17,41]

The zeta potential is a crucial indicator of the surface charge of particles. Higher zeta potential values signify stronger repulsive forces between particles, thereby enhancing the LPs stability.[42] LPs are considered "stable when their zeta potential is greater than +30 mV or lower than −30 mV".[43] In this study, all the formulated liposomes exhibited a sufficiently high zeta potential, suggesting robust electrostatic repulsion and long-term stability against coagulation and aggregation. As shown in Table 3, the zeta potential varied between −28.812 mV in the control sample (C_0) and −43.021 mV in bilayer liposomes. Differences in liposomal charge may result from electrostatic interactions between charged particles and the surface.[44] A higher sterol concentration resulted in a significant ($p < 0.05$) reduction in net surface charge, implying that phytosterol partially replaces charged phospholipids, decreasing the

Table 3 Effect of wall materials on EE, particle size, zeta potential and PDI of liposomes

Sample	Soy lecithin (%)	β-Sitosterol (%)	FD-CALE (% w/w)	Encapsulation efficiency (%)	Particle size (μm)	PDI	Zeta potential (mV)
C0	100	0	10	60.360 ± 0.780^{b}	443.738 ± 10.246^{a}	0.182 ± 0.002^{a}	-28.812 ± 1.825^{d}
C1	90	10	10	67.875 ± 0.570^{c}	597.102 ± 10.007^{b}	0.176 ± 0.002^{a}	-34.526 ± 1.132^{bc}
C2	80	20	10	73.939 ± 0.713^{d}	607.911 ± 12.702^{bc}	0.194 ± 0.001^{b}	-43.021 ± 0.761^{a}
C3	70	30	10	74.789 ± 0.811^{d}	634.115 ± 9.773^{e}	0.208 ± 0.002^{c}	-36.277 ± 1.922^{b}
C4	60	40	10	69.470 ± 1.416^{c}	661.179 ± 10.215^{d}	0.253 ± 0.003^{d}	-34.055 ± 0.782^{bc}
C5	50	50	10	55.372 ± 0.947^{a}	692.695 ± 10.126^{cd}	0.267 ± 0.003^{e}	-31.303 ± 0.985^{cd}

Different letters in superscript within columns indicates significant differences established at $p < 0.05$ according to Tukey test.

surface charge. This occurs because sterol molecules form hydrogen bonds with the phospholipid head groups while strengthening hydrophobic interactions with fatty acyl chains, ultimately stabilizing the bilayer structure.[32]

Encapsulation efficiency (EE) is a key factor in evaluating the performance of nanocarriers in improving the "stability and preservation of nutrients and pharmaceutical substances".[45] It represents the percentage of bioactive compounds effectively encapsulated compared to those located on or near the surface. As indicated in Table 2, the EE for various formulations varied between 55.372% and 74.789%. The highest encapsulation efficiency (74.789 ± 0.811%) was observed when 30% βS was incorporated. However, increasing the βS content to 50% reduced EE (55.372 ± 0.947%), comparable to formulations lacking βS. This decline in EE at higher phytosterol concentrations may be attributed to reduced membrane fluidity. Excessive phytosterol content disrupts the flexibility of the phospholipid membrane, making the liposomal structure less stable and increasing the likelihood of core material leakage, ultimately lowering EE.[46] The reduced EE in liposomes containing 50% βS suggests that the vesicles may have rigid membranes that hinder their stability, leading to the escape of bioactive compounds from the "hydrophobic region".[47] Since sample 4 (C3) demonstrated the highest capacity to encapsulate bioactive compounds from CALE, along with a stable polydispersity index (PDI) and zeta potential, it was selected for further analysis.

3.3 FTIR and morphological characteristics of liposomes

FTIR analysis was performed to investigate the "secondary structures of lecithin, β-sitosterol, empty liposomes, and LP-βS (C3)" (Fig. 1). The initial peak corresponds to the FTIR spectrum of soy lecithin, where the bands near 1200 cm^{-1} and 970 cm^{-1} are attributed to P=O stretching and P–O–C vibrations. Likewise, the spectral region between 1200 and 1050 cm^{-1} represents P=O, P–O–C, and C–O–C stretching, while the absorption bands in the 1770–1500 cm^{-1} range signify OH bending vibrations. The spectral region spanning 1765–1720 cm^{-1} corresponds to "C=O vibrations".[48] The "absorption peak" at 1738.52 cm^{-1} is linked to the stretching vibration of the C=O found in "carboxylates of saturated fatty acids". Peaks in the 3000–2800 cm^{-1} range confirm CH_2 stretching vibrations, whereas the peak at 2925 cm^{-1} arises from methylene bending vibrations in fatty acids.[49] Additionally, "the absorption peak at 1465 cm^{-1} is associated with methyl group bending vibrations, while the peak at 1223 cm^{-1} corresponds to P=O stretching" in phosphate ester groups present in lecithin [50] Moreover, an "absorption peak at 2935 cm^{-1} corresponds to the stretching vibration" of the $-CH_3$ bond, whereas those at 1637 cm^{-1} and 1465 cm^{-1} are linked to C=C double bond stretching and $-CH_3$ vibrations, respectively. The "peak observed at 838 cm^{-1} represents the stretching vibration of C–O–C bonds".[51] A redshift at 1246 cm^{-1} in the liposome spectrum suggests an "elongation of the P=O bond within the polar head of the phospholipid and the C=O bond in the ester group".[52] Finally, comparing LP-βS (C3) with empty liposomes showed no distinct bioactive compound signals, signifying the successful incorporation of these compounds into the liposomal structure, thereby confirming its functional integrity.

The SEM images provided insights into the surface morphology of FD CALE (Fig. 2a) and LP-βS (C3) (Fig. 2b), while Fig. 2c presents the microscopic view of LP-βS (C3). Fig. 1a shows wrinkled surfaces, which can be attributed to the sample's rapid shrinkage during the cooling process of the freeze–drying stage. Additionally, the surface of the freeze–dried CALE appeared rough and uneven. The dried liposomes exhibited a smooth and intact surface, showing no signs of deformation. The interaction between βS and lecithin led to

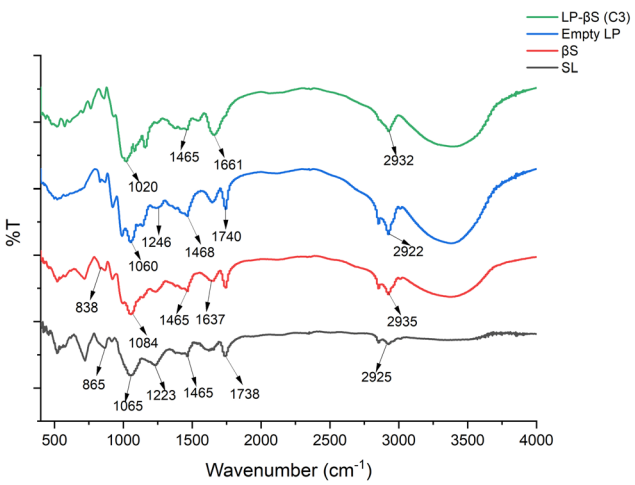

Fig. 1 FTIR spectrum all the samples.

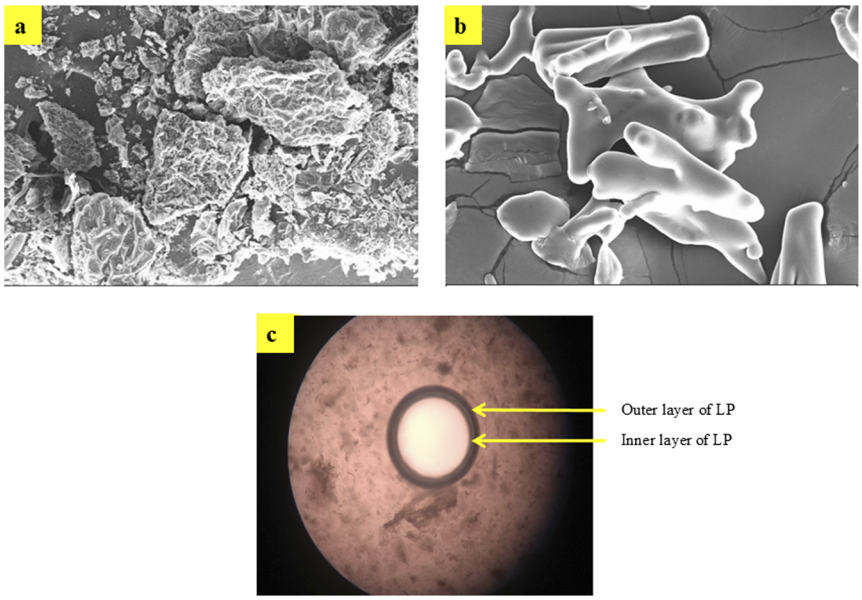

Fig. 2 Scanning electron microscope image of (a) FD CALE, (b) LP-βS (C3) and (c) LP-βS (C3) under optic microscope. Abbreviations: FD CALE: freeze-dried *Centella asiatica* leaf extract; LP-βS (C3): encapsulated sample with soy lecithin to β-sitosterol (βS) at the ratio of 7 : 3.

forming a compact and irregular structure due to cross-linking. Additionally, no visible cracks or pores were observed on the external surface of the liposomes, indicating that the core material remained securely encapsulated. The microscopic analysis further confirmed the formation of liposomes with a well-defined bilayer structure, free from any breakages or structural defects.

3.4 Retention rate of bioactive compounds and kinetics during storage

Liposomes play a crucial role in safeguarding bioactive compounds during storage, directly impacting their "effectiveness as a delivery system". As shown in Fig. 3, the total phenolic content (TPC) of LP-βS (C3) exhibited minimal variation throughout 28 days of storage at 4 °C, suggesting the stability of the liposomes. This stability is likely due to the elevated concentration of bioactive compounds, which enhance the integrity of the phospholipid membrane and reduce the leakage of encapsulated extracts within the hydrophilic core. Additionally, the bioactive compounds interact with reactive sites on lipids and βS, reducing their escape from the bilayer.[41] These results align with Zhao *et al.*, who observed minimal changes in liposome-encapsulated active compounds over storage periods.[53] As seen in Fig. 3, the retention of bioactive compounds in both FD-CALE and LP-βS (C3) declined over time. However, among the samples stored at 4 °C, FD-CALE exhibited less degradation than LP-βS (C3), while the most significant deterioration occurred in FD-CALE stored at 27 °C. These findings suggest that liposomal encapsulation effectively preserves TPC and antioxidant properties, whereas storage at ambient temperatures accelerates bioactive compound degradation in both formulations.

To evaluate the degradation behavior of bioactive compounds in FD-CALE and LP-βS (C3), their retention rates at different storage temperatures were fitted to the first-order kinetic equation. Parameters such as half-life ($t_{1/2}$), D value (time for 90% degradation), degradation constant (k), and correlation coefficient (R^2) were determined and presented in Fig. 3. The analysis revealed that an increase in storage

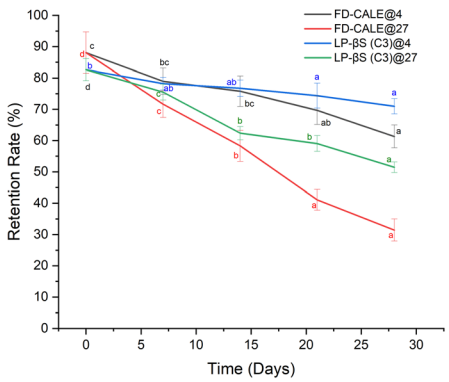

Sample	Storage Temperature (°C)	R^2	k (1/days)	$t_{1/2}$, Days	D value (Days)
FD-CALE	4	0.975	0.012	58.248	84.034
	27	0.988	0.035	19.636	28.329
LP-βS (C3)	4	0.975	0.005	138.629	200.000
	27	0.978	0.017	40.535	58.480

Fig. 3 Retention rate of bioactive compounds in FD-CALE and LP-βS (C3) during storage and their corresponding first order kinetics parameters. Abbreviations: FD-CALE: freeze dried *Centella asiatica* leaf extract; LP-βS (C3): encapsulated sample with soy lecithin to β-sitosterol (βS) at the ratio of 7 : 3.

temperature resulted in a higher degradation constant (k), likely due to enhanced molecular collisions at elevated temperatures.[31,32] Among the samples, LP-βS (C3) stored at 4 °C exhibited the most extended half-life (138.629 days), significantly outlasting FD-CALE (58.248 days) under the same conditions. Similarly, the D value was higher for encapsulated bioactive compounds than their non-encapsulated counterparts, suggesting that LP-βS (C3) offers a prolonged shelf life. The synergistic effect of SL and βS plays a vital role in protecting bioactive compounds from moisture and heat, thereby reducing degradation in LP-βS (C3).

3.5. Thermal stability

Fig. 4a illustrates the varying retention rates of bioactive compounds (BACs) in freeze-dried *Centella asiatica* leaf extract (FD-CALE) and liposomal β-sitosterol formulation (LP-βS (C3)) when exposed to different heat treatment durations and temperatures: 35 °C for 6 hours, 65 °C for 25 min, and 90 °C for 30 s. The FD-CALE exhibited rapid BAC degradation, retaining only 14.77% of its initial content after 25 min at 65 °C. In contrast, LP-βS (C3) demonstrated significantly improved thermal stability, preserving over 70% of BACs under the same conditions. Including β-sitosterol in the liposomes further mitigated BAC degradation, enhancing protection. This effect is primarily attributed to the deeper incorporation of BACs within the bilayer structure, reducing leakage due to the denser molecular packing and the more organized multi-lamellar vesicular arrangement. Similarly, a study by Tai *et al.* on the thermal stability of curcumin in Cur-LP revealed that incorporating 50 mol% of βS provided the highest thermal stability within the initial 30 min of exposure.[22]

3.6 Lipid oxidation during storage

"Lipid oxidation was evaluated using the TBARS assay, which measures the formation of malondialdehyde (MDA)" as a byproduct of unsaturated fatty acid degradation. As depicted in Fig. 4b, fluctuations in thiobarbituric acid levels in LP-βS (C3) were tracked at 4 °C and 27 °C over 28 days. Bioactive compounds significantly slowed the oxidation process ($P < 0.05$). A comparison of LP-βS (C3) stored at different temperatures revealed that liposomes maintained at 4 °C exhibited superior oxidative stability compared to those kept at 27 °C. These findings indicate that lower storage temperatures enhance oxidative stability. Lipid oxidation likely occurs "due to the accumulation of secondary oxidation" products during the formulation of liposomes. The "higher MDA equivalent" values in liposomes stored at lower temperatures suggest that encapsulating a phenolic compound with potent antioxidant properties may effectively mitigate lipid oxidation in LP-βS (C3) at 4 °C. This protective effect is likely "due to the antioxidant activity of the core material", which may influence "the lipid bilayer by limiting oxygen interaction with the membrane".[54] Similar results were reported by Vergara *et al.*, who found that encapsulating lactoferrin in liposomes led to a decrease in MDA levels over a 30 day storage period.[48] The subsequent reduction in MDA concentration after reaching a peak may be linked to the depletion of fatty acids necessary for MDA formation.[48]

3.7. *In vitro* release study

Following the simulated three-phase gastrointestinal digestion process, the release of encapsulated bioactive compounds (BACs) was evaluated. It is well established that digestive enzymes and bile salts are crucial in disrupting nanocarriers, thereby influencing nutrient absorption by small intestinal epithelial cells.[55] As illustrated in Fig. 5, encapsulated BACs in gastric fluid were released slowly. However, the "cumulative release rate" of BACs in FD-CALE was more significant than encapsulated BACs. The enhanced stability of LP-βS (C3) likely minimizes interactions between BACs and digestive compounds, preventing premature degradation and release before reaching the intestinal phase.[56] Furthermore, the infiltration of bile salts increases the fluidity of the phospholipid membrane in liposomes, consequently accelerating the release of BACs.[41] The findings also revealed that BACs were released at

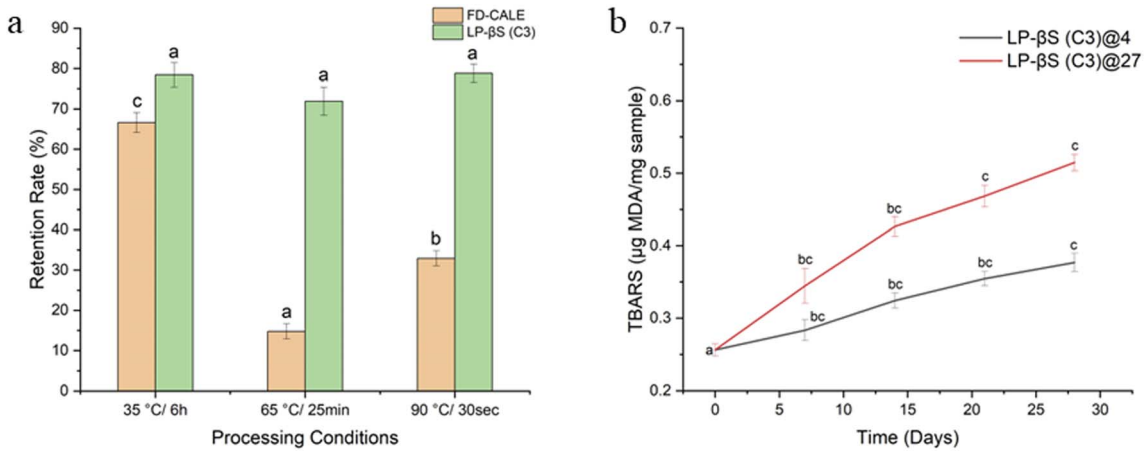

Fig. 4 (a) Thermal stability of FD-CALE and LP-βS (C3) under different processing conditions and (b) lipid oxidation in LP-βS (C3) under different storage period temperatures. Abbreviations: FD-CALE: freeze dried *Centella asiatica* leaf extract; LP-βS (C3): encapsulated sample with soy lecithin to β-sitosterol (βS) at the ratio of 7 : 3.

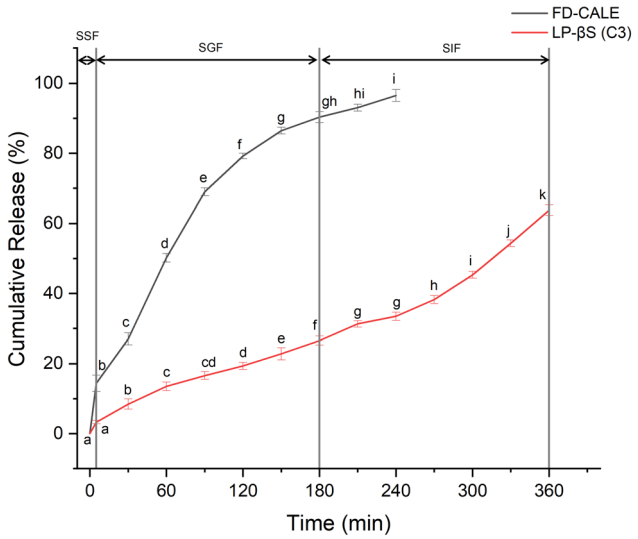

Fig. 5 Cumulative release of BACs during *in vitro* release study. Abbreviations: BACs: bioactive compounds.

a slower rate in the "stomach (8.454 ± 1.482 to 26.538 ± 1.289%) than in the small intestine (26.538 ± 1.289 to 63.766 ± 1.521%)", indicating that the "layer-by-layer self-assembled liposomes" effectively shield BACs in the gastric environment while promoting their release in the intestinal phase, thereby enhancing bio-accessibility. Similar observations were reported by Tai *et al.*[22] Thus, including βS significantly improves the bioavailability of CALE BACs in liposomes.

4 Conclusions

This study employed LC-MS/MS analysis to identify bioactive compounds (BACs) in *Centella asiatica* leaf extract (CALE). Liposomes (LP) incorporating varying concentrations of β-sitosterol (βS) were also successfully formulated. The inclusion of βS enhanced the stability and bioavailability of LP-βS. Its presence facilitated strong intermolecular interactions, forming a compact and stable liposomal structure. Findings revealed that freeze-dried CALE (FD-CALE) exhibited instability, whereas applying a coating improved liposome's physical stability. Retention rate kinetics demonstrated that LP-βS (C3) effectively preserved bioactive compounds at a low temperature (4 °C), with a calculated half-life of 138.63 days. Evaluation of oxidation indices indicated that oxidative compound levels in LP-βS (C3) were lower than those in FD-CALE, with the liposomal bilayer coating playing a crucial role in reducing oxidation. Furthermore, liposomes effectively retain core bioactivity even under short-term exposure to high temperatures. Thus, the encapsulation of polyphenol-rich CALE within liposomes was successfully achieved. *In vitro* release studies demonstrated a delayed release of BACs in the gastrointestinal tract (GIT) when βS was incorporated into the liposomal formulation.

Data availability

The data will be available on request.

Author contributions

Soubhagya Tripathy: conceptualization; data curation; formal analysis; methodology; validation; writing – original draft; writing – review & editing, Prem Prakash Srivastav: conceptualization; supervision; validation; visualization; writing – review & editing.

Conflicts of interest

The authors declare no conflict of interest.

Acknowledgements

The author, Soubhagya Tripathy thanks the Ministry of Education (formerly the Ministry of Human Resource Development), Government of India for an Institute Research Assistantship, and thanks to the Agricultural and Food Engineering Department, Indian Institute of Technology Kharagpur for their assistance in this study.

References

1 K. Banwo, A. O. Olojede, A. T. Adesulu-Dahunsi, D. K. Verma, M. Thakur, S. Tripathy, *et al.*, Functional importance of bioactive compounds of foods with potential health benefits: A review on recent trends, *Food Biosci*, 2021, **43**, 101320, DOI: 10.1016/j.fbio.2021.101320.

2 A. Narayanankutty, A. C. Famurewa and E. Oprea, Natural bioactive compounds and human health, *Molecules*, 2024, **29**(14), 3372.

3 C. S. Riar and P. S. Panesar, Bioactive compounds and nutraceuticals: Classification, potential sources, and application status, in *Bioactive Compounds and Nutraceuticals from Dairy, Marine, and Nonconventional Sources*, Apple Academic Press, 2024, pp. 3–60.

4 S. Tripathy, D. K. Verma, M. Thakur, N. Chakravorty, S. Singh and P. P. Srivastav, Recent trends in extraction, identification and quantification methods of Centella asiatica phytochemicals with potential applications in food industry and therapeutic relevance: A review, *Food Biosci.*, 2022, **49**, 101864.

5 S. Tripathy and P. P. Srivastav, Synergistic effects of dielectric barrier discharge (DBD) cold plasma pretreatment combined with microwave drying on the physicochemical and functional properties of Centella asiatica leaves, *Food Bioprocess Technol.*, 2024, **17**(11), 3979–3998.

6 S. Nakra, S. Tripathy and P. P. Srivastav, Green and Sustainable Extraction of Bioactive Compounds from Centella asiatica leaves using Microwave Pretreatment and Ultrasonication: Kinetics, Process Optimization, and Biological Activity, *Food Biophys.*, 2025, **20**(1), 1–18.

7 P. Mohapatra, A. Ray, S. Jena, B. M. Padhiari, A. Kuanar, S. Nayak and S. Mohanty, Artificial neural network based prediction and optimization of centelloside content in Centella asiatica: A comparison between multilayer perceptron (MLP) and radial basis function (RBF)

algorithms for soil and climatic parameter, *S. Afr. J. Bot.*, 2023, **160**, 571–585.
8 H. Amiri, B. Shabanpour and P. Pourashouri, Encapsulation of marine bioactive compounds using liposome technique: Evaluation of physicochemical properties and oxidative stability during storage, *Food Struct.*, 2023, **35**, 100308, DOI: 10.1016/j.foostr.2023.100308.
9 S. Tripathy, D. K. Verma, A. K. Gupta, P. P. Srivastav, A. R. Patel, M. L. C. González and C. N. Aguilar, Nanoencapsulation of biofunctional components as a burgeoning nanotechnology-based approach for functional food development: a review, *Biocatal. Agric. Biotechnol.*, 2023, **53**, 102890.
10 M. Rakshit, S. Tripathy and P. P. Srivastav, Encapsulation of natural polyphenols for food applications, in *Novel Processing Methods for Plant-Based Health Foods*, Apple Academic Press, 2023, pp. 123–162.
11 D. D. Milinčić, A. S. Salević-Jelić, A. Ž. Kostić, S. P. Stanojević, V. Nedović and M. B. Pešić, Food nanoemulsions: how simulated gastrointestinal digestion models, nanoemulsion, and food matrix properties affect bioaccessibility of encapsulated bioactive compounds, *Crit. Rev. Food Sci. Nutr.*, 2024, **64**(22), 8091–8113.
12 B. Liu, L. Zan, X. Li, Y. Cai and G. Hao, Modification of liposomes: Preparation, purpose, methods and the application in food, *Int. J. Food Sci. Technol.*, 2024, **59**(6), 3523–3536.
13 J. Xiao, W. Tian, H. Abdullah, H. Wang, M. Chen, Q. Huang and Y. Cao, Updated design strategies for oral delivery systems: Maximized bioefficacy of dietary bioactive compounds achieved by inducing proper digestive fate and sensory attributes, *Crit. Rev. Food Sci. Nutr.*, 2024, **64**(3), 817–836.
14 A. G. Valdes-Becerril, R. Jimenez-Rodriguez, J. Douda, B. El Filali, I. C. Ballardo-Rodriguez and I. C. Romero-Ibarra, Co-encapsulation of Vincristine and Vitamin E in Soy Lecithin/Hydrogenated Soy Lecithin Liposomes, *Bionanosci.*, 2025, **15**(1), 164.
15 E. M. Akl, A. A. Abd-Rabou and A. F. Hashim, Anti-colorectal cancer activity of constructed oleogels based on encapsulated bioactive canola extract in lecithin for edible semisolid applications, *Sci. Rep.*, 2025, **15**, 4945, DOI: 10.1038/s41598-025-12345-6.
16 D. A. Hofmaenner, A. Kleyman, A. Press, M. Bauer and M. Singer, The many roles of cholesterol in sepsis: a review, *Am. J. Respir. Crit. Care Med.*, 2022, **205**, 388–396, DOI: 10.1164/rccm.202104-0987PP.
17 C. Han, C. Yang, X. Li, E. Liu, X. Meng and B. Liu, DHA loaded nanoliposomes stabilized by β-sitosterol: Preparation, characterization and release *in vitro* and vivo, *Food Chem.*, 2022, **368**, 130859, DOI: 10.1016/j.foodchem.2021.130859.
18 A. Kontush, *Cholesterol, Lipoproteins, and Cardiovascular Health: Separating the Good (HDL), the Bad (LDL), and the Remnant*, John Wiley & Sons, 2024.
19 J. Vekic, A. Zeljkovic, A. F. Cicero, A. Janez, A. P. Stoian, A. Sonmez and M. Rizzo, Atherosclerosis development and progression: the role of atherogenic small, dense LDL, *Medicina*, 2022, **58**(2), 299.
20 X. Li, Y. Xin, Y. Mo, P. Marozik, T. He and H. Guo, The bioavailability and biological activities of phytosterols as modulators of cholesterol metabolism, *Molecules*, 2022, **27**(2), 523.
21 A. Poudel, G. Gachumi, P. G. Paterson, A. El-Aneed and I. Badea, Liposomal phytosterols as LDL-cholesterol-lowering agents in diet-induced Hyperlipidemia, *Mol. Pharm.*, 2023, **20**(9), 4443–4452.
22 K. Tai, M. Rappolt, X. He, Y. Wei, S. Zhu, J. Zhang and F. Yuan, Effect of β-sitosterol on the curcumin-loaded liposomes: Vesicle characteristics, physicochemical stability, *in vitro* release and bioavailability, *Food Chem.*, 2019, **293**, 92–102.
23 A. A. Jovanović, B. D. Balanč, A. Ota, P. Ahlin Grabnar, V. B. Djordjević, K. P. Šavikin, *et al.*, Comparative effects of cholesterol and β-sitosterol on the liposome membrane characteristics, *Eur. J. Lipid Sci. Technol.*, 2018, **120**(9), 1800039.
24 R. Upadhyay, G. Nachiappan and H. N. Mishra, Ultrasound-assisted extraction of flavonoids and phenolic compounds from Ocimum tenuiflorum leaves, *Food Sci. Biotechnol.*, 2015, **24**, 1951–1958.
25 R. Sabaragamuwa and C. O. Perera, Total triterpenes, polyphenols, flavonoids, and antioxidant activity of bioactive phytochemicals of Centella asiatica by different extraction techniques, *Foods*, 2023, **12**(21), 3972.
26 S. M. Singh, S. Tripathy and P. P. Srivastav, Bioactive compound extraction from giloy leaves and steam using ultrasound: bioactivity, antimicrobial, and LC–MS/MS study, *Food Sci. Biotechnol.*, 2025, 1–13.
27 G. Prevete, E. Donati, A. P. Ruggiero, S. Fardellotti, L. Lilla, V. Ramundi, *et al.*, Encapsulation of Olea europaea Leaf Polyphenols in Liposomes: A Study on Their Antimicrobial Activity to Turn a Byproduct into a Tool to Treat Bacterial Infection, *ACS Appl. Mater. Interfaces*, 2024, **16**(50), 68850–68863.
28 R. D. Păvăloiu, F. Sha'at, G. Neagu, M. Deaconu, C. Bubueanu, A. Albulescu, *et al.*, Encapsulation of polyphenols from Lycium barbarum leaves into liposomes as a strategy to improve their delivery, *Nanomaterials*, 2021, **11**(8), 1938.
29 M. A. Hashim, X. Huang, L. A. Nadtochii, D. A. Baranenko, M. S. Boulkrane and T. M. El-Messery, Encapsulation of bioactive compounds extracted from date palm seeds (Phoenix dactylifera L.) and their use in functional food, *Front. Nutr.*, 2022, **9**, 1051050, DOI: 10.3389/fnut.2022.1051050.
30 S. Tripathy and P. P. Srivastav, Effect of dielectric barrier discharge (DBD) cold plasma-activated water pre-treatment on the drying properties, kinetic parameters, and physicochemical and functional properties of Centella asiatica leaves, *Chemosphere*, 2023, **332**, 138901.
31 C. C. Ariahu, O. S. Kamaldeen and M. I. Yusufu, Kinetic and thermodynamic studies on the degradation of carotene in

carrot powder beads, *J. Food Eng.*, 2021, **288**, 110145, DOI: 10.1016/j.jfoodeng.2020.110145.
32 S. Tripathy and P. P. Srivastav, Encapsulation of Centella asiatica leaf extract in liposome: Study on structural stability, degradation kinetics and fate of bioactive compounds during storage, *Food Chem. Adv.*, 2023, **2**, 100202.
33 C. Fan, T. Feng, X. Wang, S. Xia and C. J. Swing, Liposomes for encapsulation of liposoluble vitamins (A, D, E and K): Comparation of loading ability, storage stability and bilayer dynamics, *Food Res. Int.*, 2023, **163**, 112264, DOI: 10.1016/j.foodres.2022.112264.
34 H. S. Long, M. A. Stander and B. E. Van Wyk, Notes on the occurrence and significance of triterpenoids (asiaticoside and related compounds) and caffeoylquinic acids in Centella species, *S. Afr. J. Bot.*, 2012, **82**, 53–59.
35 A. Alqahtani, W. Tongkao-on, K. M. Li, V. Razmovski-Naumovski, K. Chan and G. Q. Li, Seasonal variation of triterpenes and phenolic compounds in Australian Centella asiatica (L.) Urban, *Phytochem. Anal.*, 2015, **26**, 436–443.
36 F. Abas, A. Khatib, K. Shaari and N. H. Lajis, Chemical characterization and antioxidant activity of three medicinal Apiaceae species, *Ind. Crops Prod.*, 2014, **55**, 238–247.
37 J. Oszmiański, A. Wojdyło, J. Gorzelany and I. Kapusta, Identification and characterization of low molecular weight polyphenols in berry leaf extracts by HPLC-DAD and LC-ESI/MS, *J. Agric. Food Chem.*, 2011, **59**, 12830–12835.
38 N. E. Gray, A. A. Magana, P. Lak, K. M. Wright, J. Quinn, J. F. Stevens, *et al.*, Centella asiatica: phytochemistry and mechanisms of neuroprotection and cognitive enhancement, *Phytochem. Rev.*, 2018, **17**, 161–194.
39 F. Zakaria, W. N. W. Ibrahim, I. S. Ismail, H. Ahmad, N. Manshoor, N. Ismail, *et al.*, LCMS/MS metabolite profiling and analysis of acute toxicity effect of the ethanolic extract of Centella asiatica on zebrafish model, *Pertanika J. Sci. & Technol.*, 2019, **27**(2), 985–1003.
40 F. F. Song, S. J. Tian, G. L. Yang and X. Y. Sun, Effect of phospholipid/flaxseed oil ratio on characteristics, structure change, and storage stability of liposomes, *LWT*, 2022, **157**, 113040.
41 X. Tan, Y. Liu, B. Shang, M. Geng and F. Teng, Layer-by-layer self-assembled liposomes fabricated using sodium alginate and chitosan: Investigation of co-encapsulation of folic acid and vitamin E, *Int. J. Biol. Macromol.*, 2024, **281**, 136464.
42 C. Tan, B. Feng, X. Zhang, W. Xia and S. Xia, Biopolymer-coated liposomes by electrostatic adsorption of chitosan (chitosomes) as novel delivery systems for carotenoids, *Food Hydrocoll.*, 2016, **52**, 774–784.
43 K. Jarzynska, A. Gajewicz-Skretna, K. Ciura and T. Puzyn, Predicting zeta potential of liposomes from their structure: A nano-QSPR model for DOPE, DC-Chol, DOTAP, and EPC formulations, *Comput. Struct. Biotechnol. J.*, 2024, **25**, 3–8.
44 L. Ramezanzade, S. F. Hosseini and M. Nikkhah, Biopolymer-coated nanoliposomes as carriers of rainbow trout skin-derived antioxidant peptides, *Food Chem.*, 2017, **234**, 220–229.
45 K. Sarabandi and S. M. Jafari, Effect of chitosan coating on the properties of nanoliposomes loaded with flaxseed-peptide fractions: Stability during spray-drying, *Food Chem.*, 2020, **310**, 125951.
46 Z. Wu, T. Wang, Y. Song, Y. Lu, T. Chen, P. Chen and W. Zhang, Optimization on conditions of podophyllotoxin-loaded liposomes using response surface methodology and its activity on PC3 cells, *J. Liposome Res.*, 2019, **29**(2), 133–141.
47 P. R. Karn, Z. Vanić, I. Pepić and N. Škalko-Basnet, Mucoadhesive liposomal delivery systems: the choice of coating material, *Drug Dev. Ind. Pharm.*, 2011, **37**(4), 482–488.
48 D. Vergara and C. Shene, Encapsulation of lactoferrin into rapeseed phospholipids based liposomes: Optimization and physicochemical characterization, *J. Food Eng.*, 2019, **262**, 29–38.
49 A. Ahmad and H. Ayub, Fourier transform infrared spectroscopy (FTIR) technique for food analysis and authentication, in *Nondestructive quality assessment techniques for fresh fruits and vegetables*, Springer Nature Singapore, Singapore, 2022, 103–142.
50 D. Zhang, Y. Zhang, Y. Gao, Y. Lin, C. Ding, J. Zhang and Q. Liu, Stability, bioavailability, and antimicrobial activity of garlic extract liposomes prepared from lecithin and β-sitosterol, *J. Food Meas. Char.*, 2022, **16**(2), 1383–1394.
51 P. Di Donato, V. Taurisano, A. Poli, G. G. d'Ayala, B. Nicolaus, M. Malinconico and G. Santagata, Vegetable wastes derived polysaccharides as natural eco-friendly plasticizers of sodium alginate, *Carbohydr. Polym.*, 2020, **229**, 115427, DOI: 10.1016/j.carbpol.2019.115427.
52 H. Y. Kim, J. H. Cheon, S. H. Lee, J. Y. Min, S. Y. Back, J. G. Song, *et al.*, Ternary nanocomposite carriers based on organic clay-lipid vesicles as an effective colon-targeted drug delivery system: preparation and in vitro/in vivo characterization, *J. Nanobiotechnol.*, 2020, **18**, 1–15.
53 L. Zhao, D. Wang, J. Yu, X. Wang, T. Wang, D. Yu and W. Elfalleh, Complex phospholipid liposomes co-encapsulated of proanthocyanidins and α-tocopherol: Stability, antioxidant activity and *in vitro* digestion simulation, *Food Biosci.*, 2024, **61**, 104899.
54 D. Marín, A. Alemán, P. Montero and M. C. Gómez-Guillén, Encapsulation of food waste compounds in soy phosphatidylcholine liposomes: Effect of freeze-drying, storage stability and functional aptitude, *J. Food Eng.*, 2018, **223**, 132–143.
55 C. Dima, E. Assadpour, A. Nechifor, S. Dima, Y. Li and S. M. Jafari, Oral bioavailability of bioactive compounds; modulating factors, *in vitro* analysis methods, and enhancing strategies, *Crit. Rev. Food Sci. Nutr.*, 2024, **64**, 8501–8539, DOI: 10.1080/10408398.2022.2155194.
56 Z. L. Li, S. F. Peng, X. Chen, Y. Q. Zhu, L. Q. Zou, W. Liu and C. M. Liu, Pluronics modified liposomes for curcumin encapsulation: Sustained release, stability and bioaccessibility, *Food Res. Int.*, 2018, **108**, 246–253.